Liposomal Formulation of *Fagonia arabica* L. Enhances Antithrombotic Efficacy: Phytochemical, Pharmacological, and Computational Investigations

Sarah A. Badawy,[1]* Ahmed R. Hassan,[1] Medhat W. Shafaa,[2] Ahmed Mansour,[3] Marwa S. Abu Bakr,[4] Abd El-Salam I. Mohammed[5]

[1] Medicinal and Aromatic Plants Department, Desert Research Center, El-Matariya 11753, Cairo, Egypt.

[2] Physics Department, Medical Biophysics Division, Faculty of Sciences, Helwan University, Helwan 11792, Cairo, Egypt.

[3] Department of Pharmacology and Toxicology, Faculty of Pharmacy (for Boys), Al-Azhar University, Nasr City 13129, Cairo, Egypt.

[4] Department of Pharmacognosy, Faculty of Pharmacy (for Girls), Al-Azhar University, Nasr City 11651, Cairo, Egypt.

[5] Department of Pharmacognosy, Faculty of Pharmacy (for Boys), Al-Azhar University, Nasr City 13129, Cairo, Egypt.

* Corresponding author

E-mail address: sarahahmed.2252@azhar.edu.eg (Sarah A. Badawy)

Abstract

Fagonia arabica "Dhamasa" is traditionally used in Ayurvedic and Unani medicine across South Asia and the Middle East for its therapeutic properties, notably as a natural blood purifier. It is believed to aid in dissolving blood clots and reducing the risk of brain hemorrhage and cardiovascular events. Given previous reports of saponin content in *F. arabica*, this study aimed to evaluate its thrombolytic and anticoagulant potential. After confirming its saponin richness through NMR (1D, 2D) and LC-MS, we developed liposomal nanoparticles to enhance bioavailability and target clot dissolution more effectively. Liposomes were characterized using TEM, particle size, PDI, and zeta potential. *In vitro* thrombolytic and anticoagulant activities were assessed, followed by *in vivo* testing in adult Wistar rats. The dose-dependent effects of the saponin-rich *n*-butanol fraction of *F. arabica* on Antithrombin-III levels were evaluated using an *in vitro* quantitative immunoturbidimetric assay. Coagulation parameters were evaluated using aPTT and PT assays. A molecular docking study was systematically performed on nine targets using the five structurally elucidated steroidal and terpenoid glycosides to predict and evaluate their binding affinities. These computational findings were designed to complement ongoing *in vitro* and *in vivo* investigations. The butanol extract showed significant *in vitro* thrombolytic and anticoagulant effects at 40 mg/mL. The results demonstrate that the saponin-rich fraction modulates Antithrombin-III in a concentration-dependent manner. Liposomal nanoparticles achieved similar efficacy *in vivo* at just 3 mg/kg, compared to 100 mg/kg for the non-nano extract. The liposomal group showed PT of 35 ± 4 s and aPTT >180 s, outperforming the non-nano extract (PT 30 ± 7 s, aPTT >180 s) and controls (PT 12 ± 2 s, aPTT 37 ± 3 s). The docking study provides mechanistic insight into their potential multi-target antithrombotic activities. Besides the butanol extract, liposomal *F. arabica* enhances antithrombotic efficacy at lower doses, supporting its potential as a natural therapeutic candidate for thrombotic disorders.

Keywords: *Fagonia arabica,* Dhamasa, Saponins, Anticoagulant assay, Thrombolytic assay, Liposomal nanoparticles, aPTT and PT assays.

1. Biological studies

Table S.1 *In vitro* thrombolytic effects of *F. arabica* fractions and standard controls

Sample	% Clot lysis	±SD
Normal saline	18.31	0.42
Heparin	15.575	2.155
F. arabica 80% hydro-methanolic extract	23.385	0.235
F. arabica DCM fraction	12.17	0.73
F. arabica ethyl acetate fraction	6.655	0.175
F. arabica butanol fraction	29.505	0.095
F. arabica remaining aqueous fraction	24.13	0.09

2. Phytochemical studies of the most biologically active fraction

2.1. LC-ESI-MS/MS Fragmentation of the butanol fraction

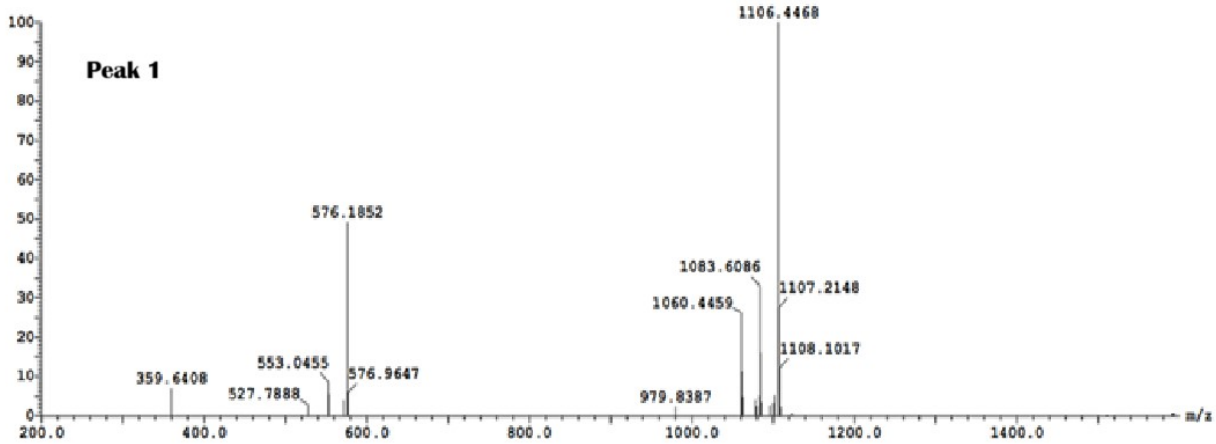

Fig. S.1. Peak 1 MS/MS fragmentation

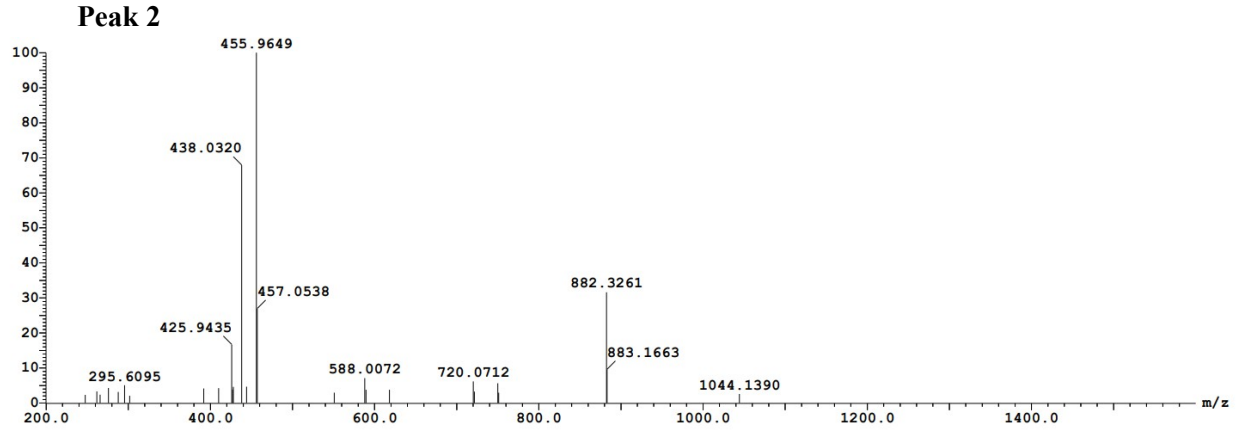

Fig. S.2. Peak 2 MS/MS fragmentation

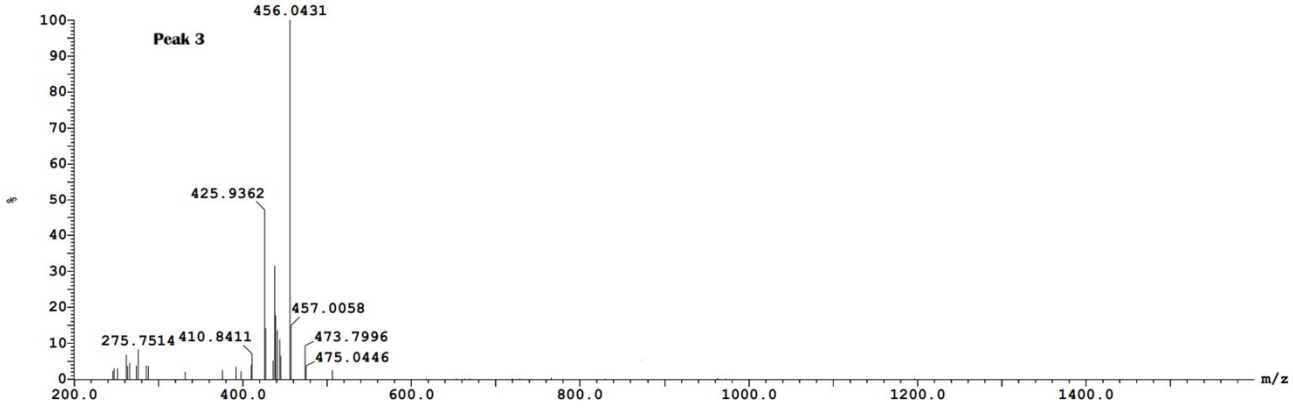

Fig. S.3. Peak 3 MS/MS fragmentation

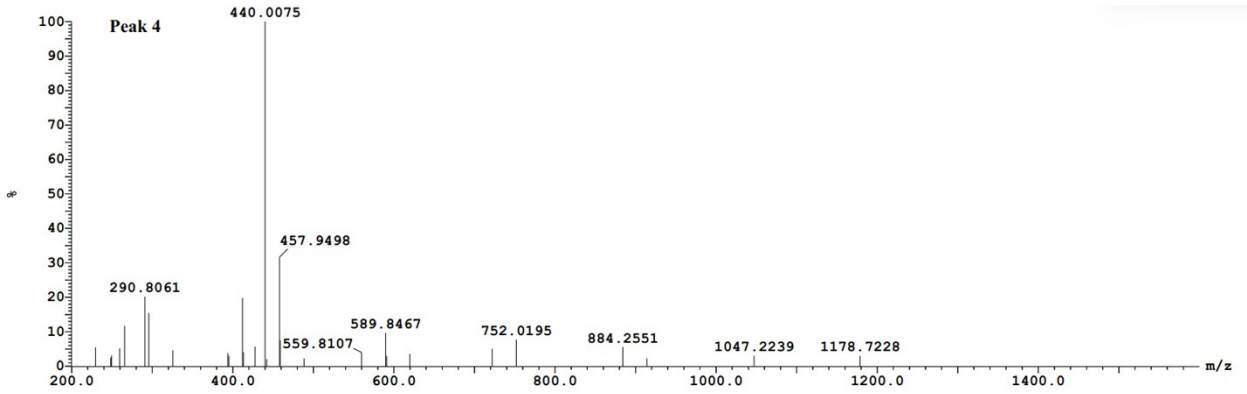

Fig. S.4. Peak 4 MS/MS fragmentation

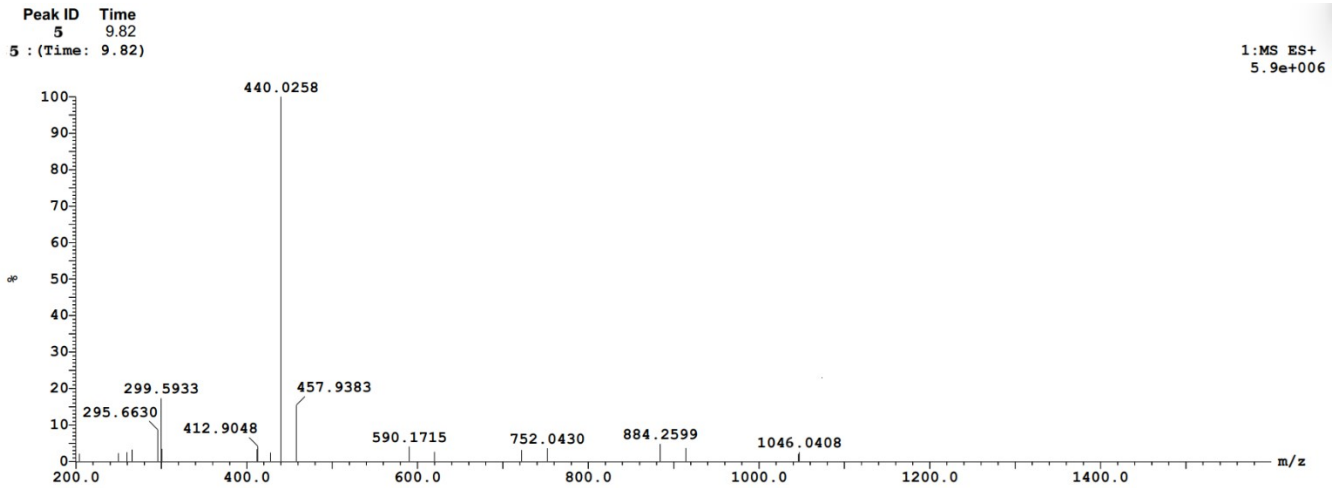

Fig. S.5. Peak 5 MS/MS fragmentation

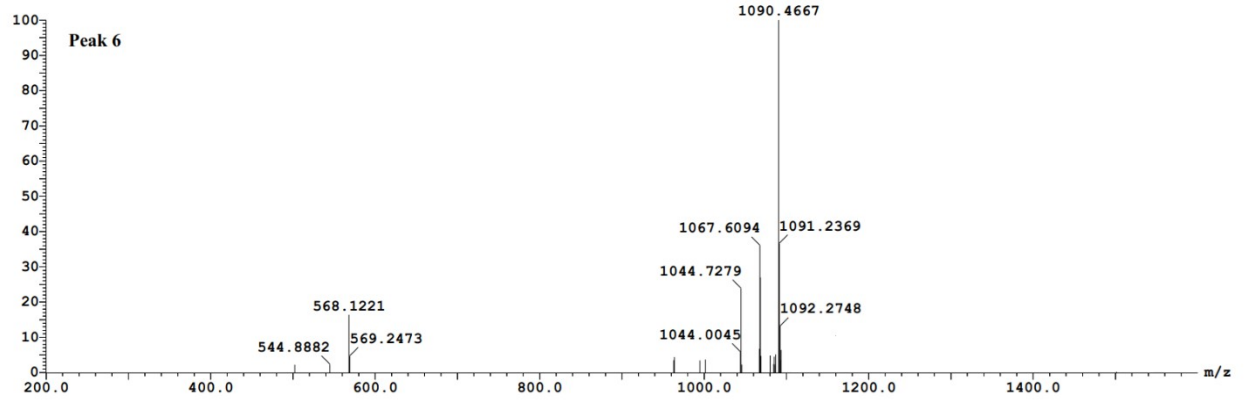

Fig. S.6. Peak 6 MS/MS fragmentation

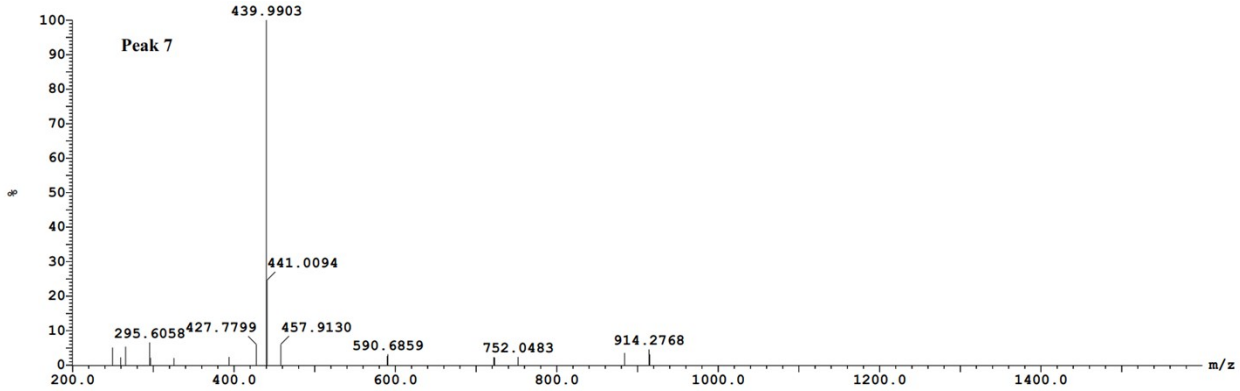

Fig. S.7. Peak 7 MS/MS fragmentation

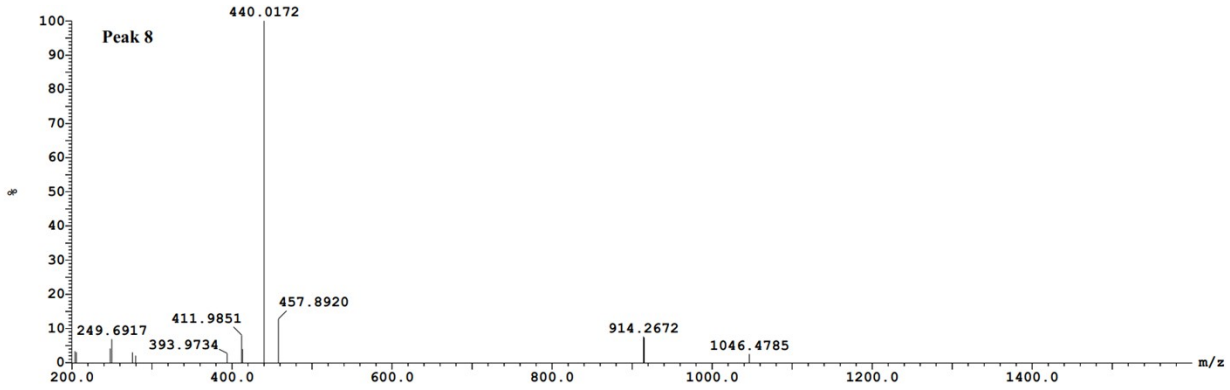

Fig. S.8. Peak 8 MS/MS fragmentation

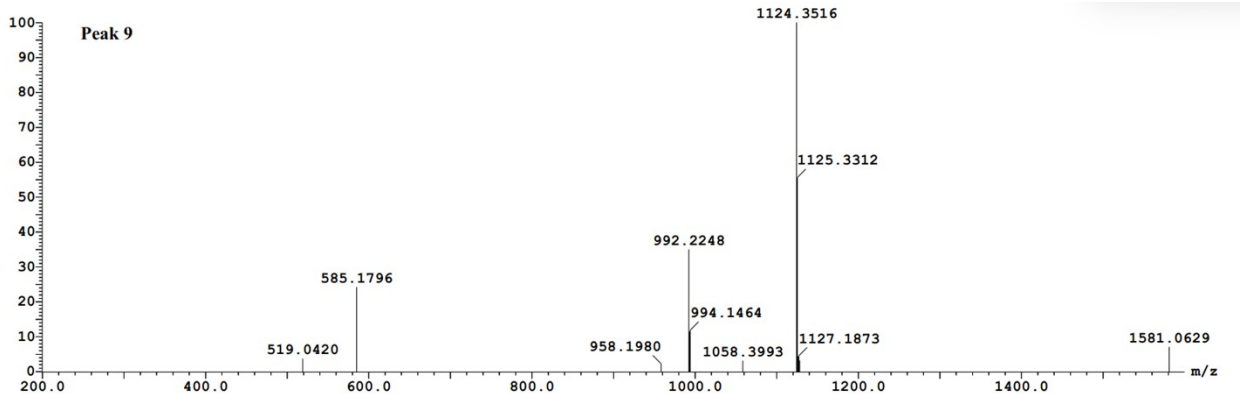

Fig. S.9. Peak 9 MS/MS fragmentation

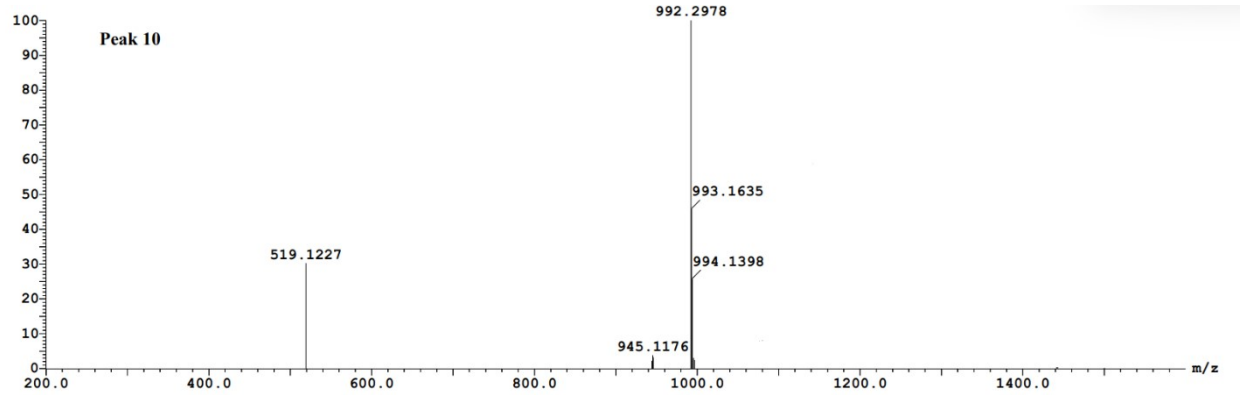

Fig. S.10. Peak 10 MS/MS fragmentation

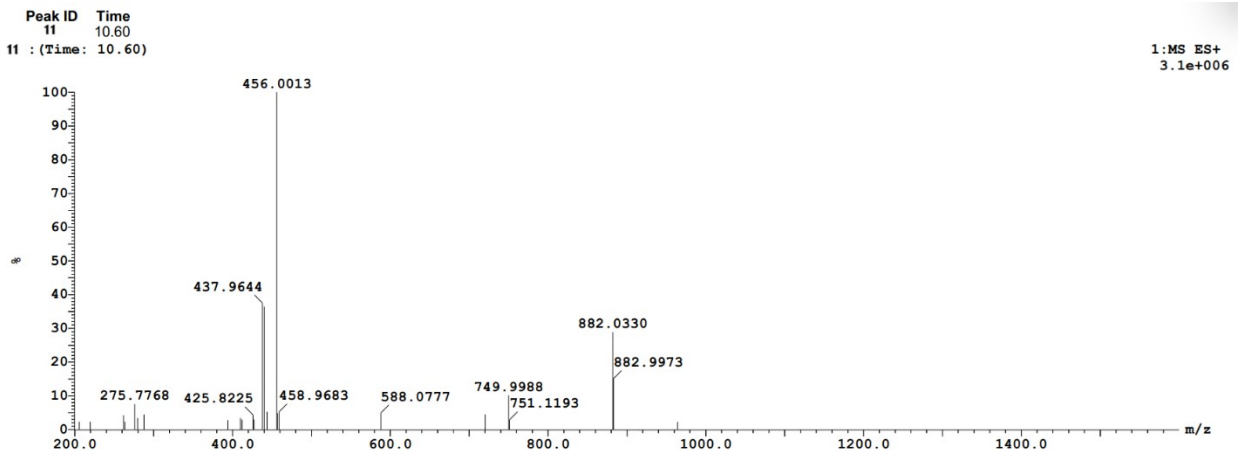

Fig. S.11. Peak 11 MS/MS fragmentation

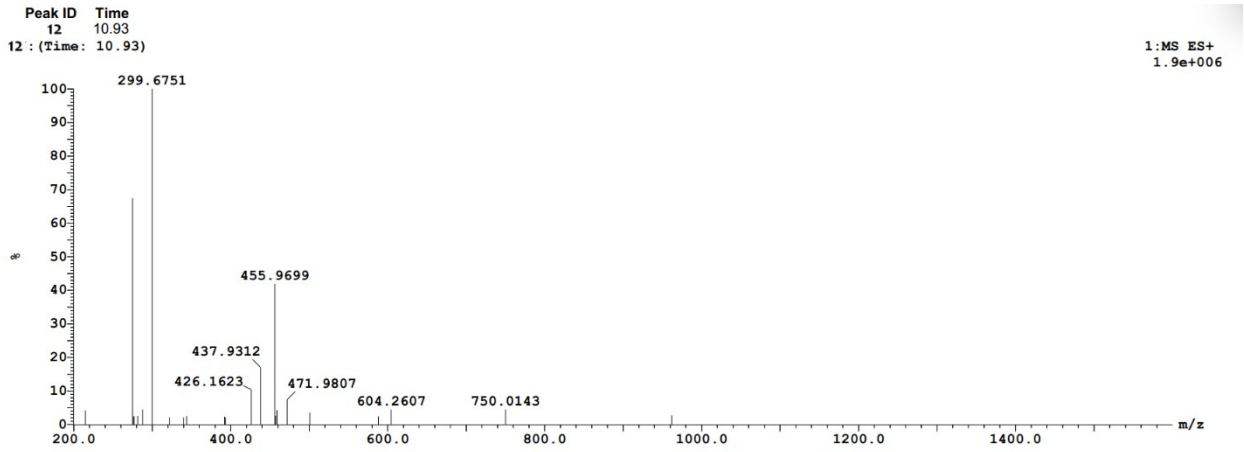

Fig. S.12. Peak 12 MS/MS fragmentation

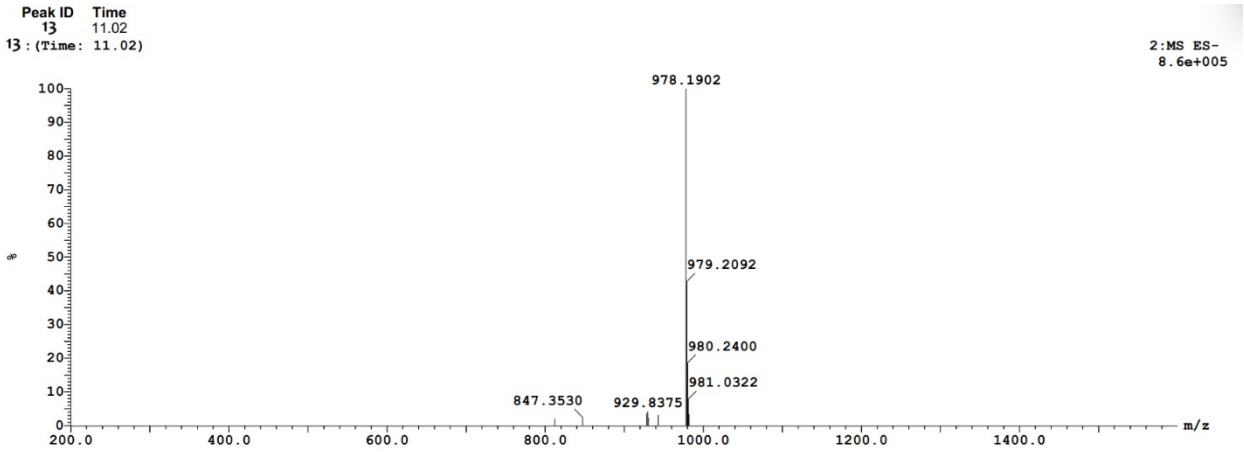

Fig. S.13. Peak 13 MS/MS fragmentation

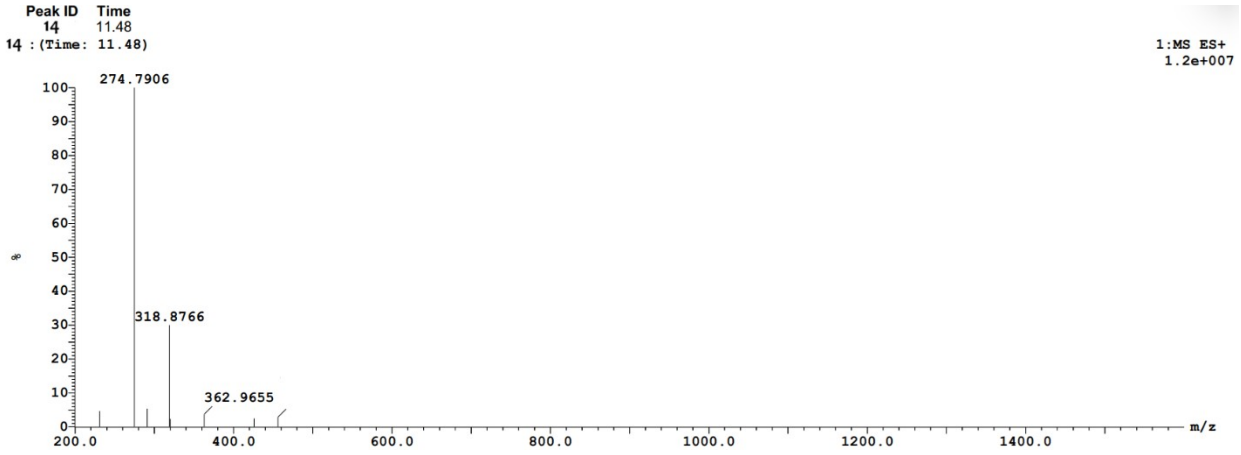

Fig. S.14. Peak 14 MS/MS fragmentation

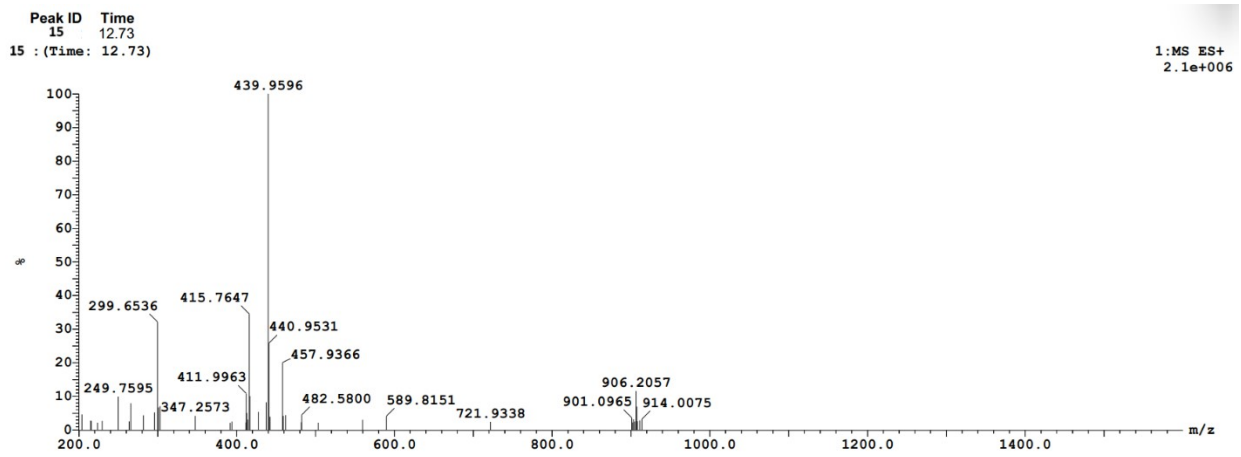

Fig. S.15. Peak 15 MS/MS fragmentation

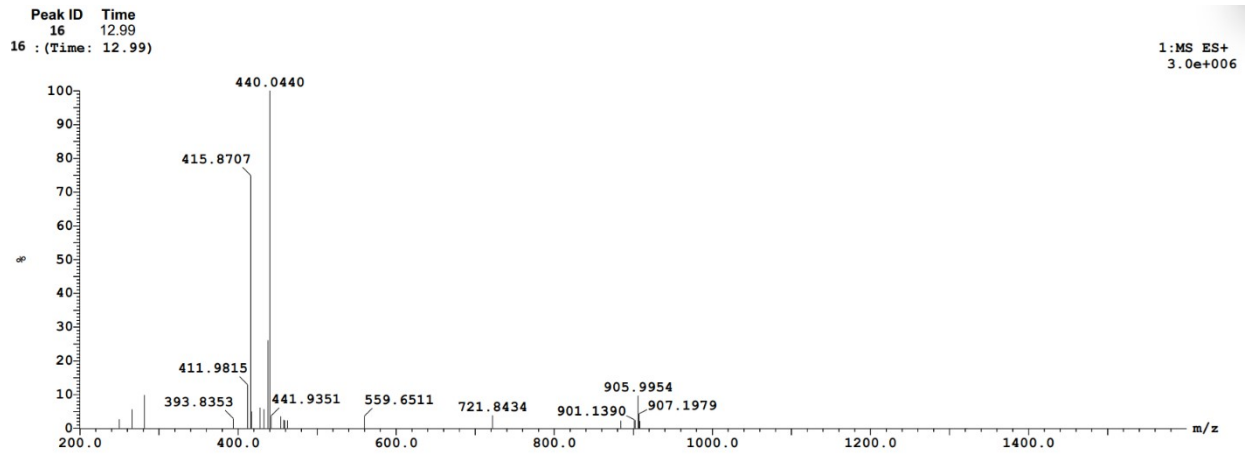

Fig. S.16. Peak 16 MS/MS fragmentation

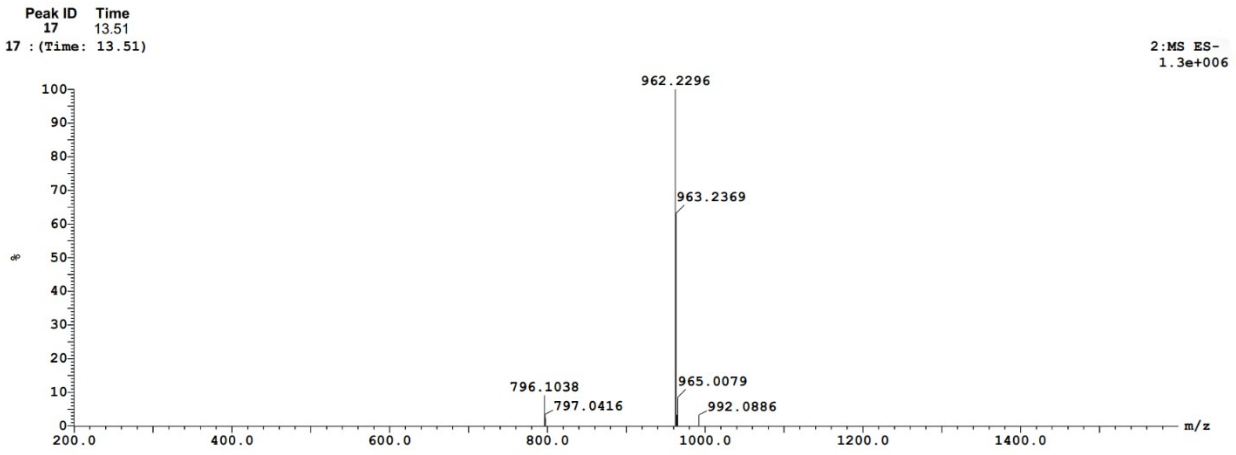

Fig. S.17. Peak 17 MS/MS fragmentation

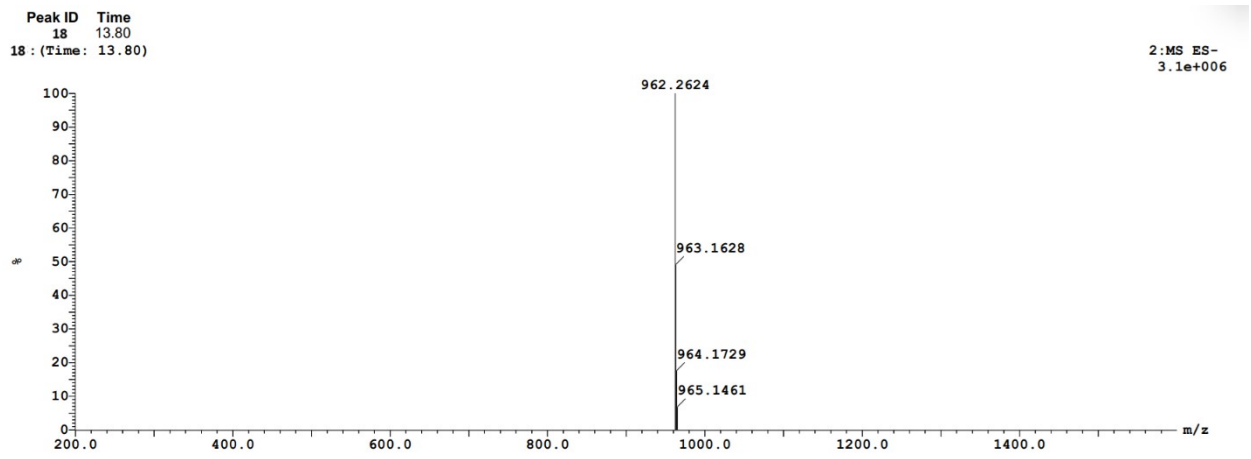

Fig. S.18. Peak 18 MS/MS fragmentation

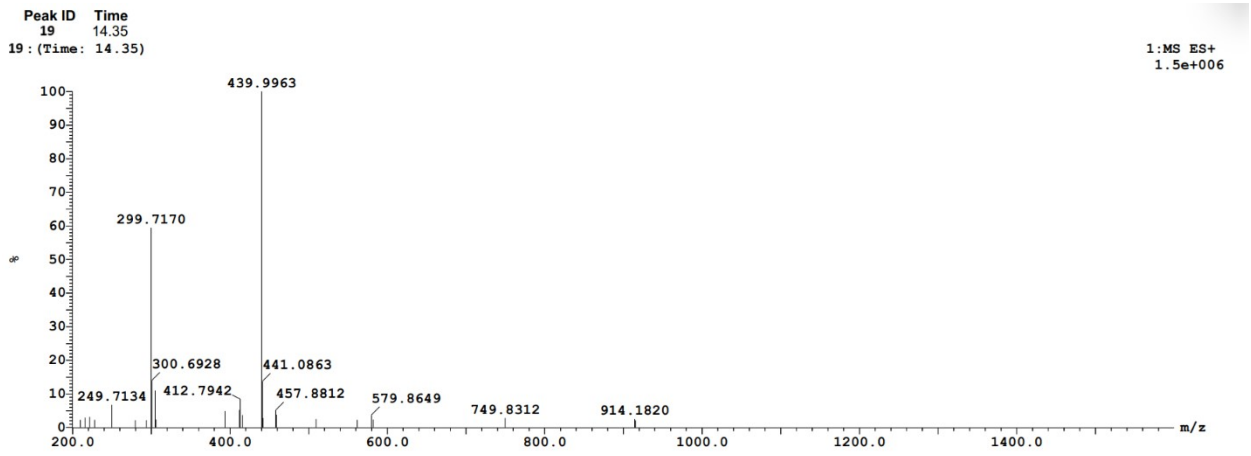

Fig. S.19. Peak 19 MS/MS fragmentation

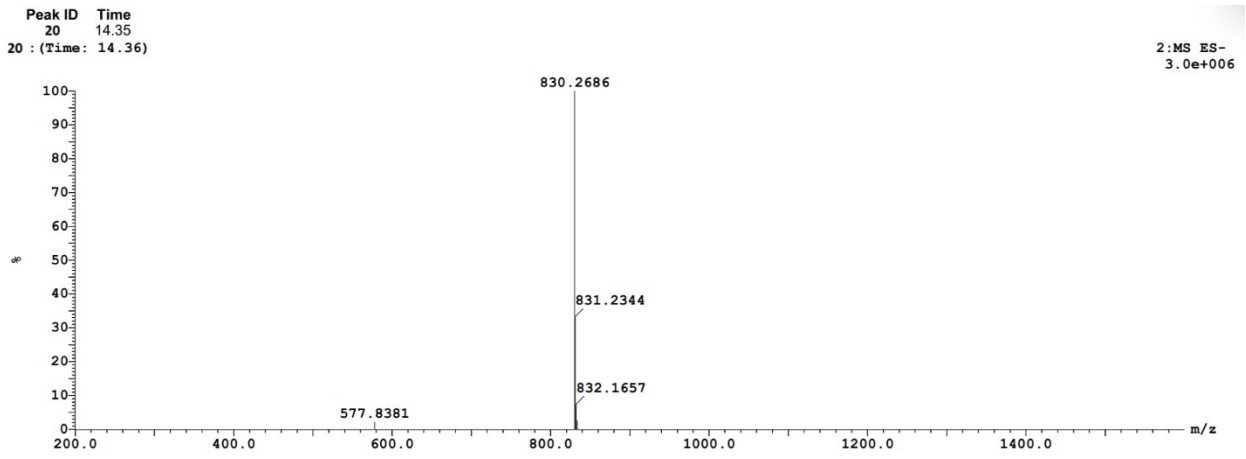

Fig. S.20. Peak 20 MS/MS fragmentation

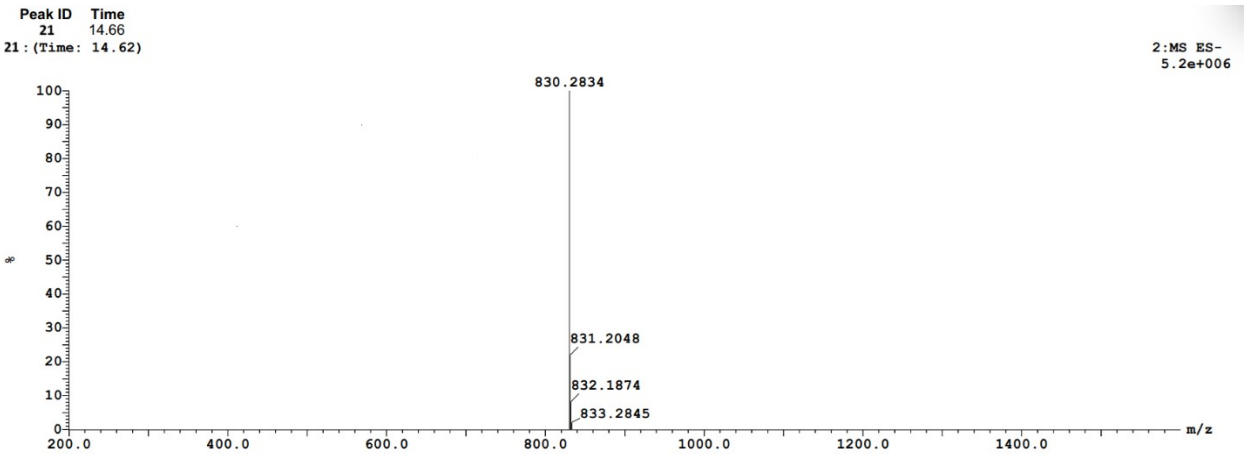

Fig. S.21. Peak 21 MS/MS fragmentation

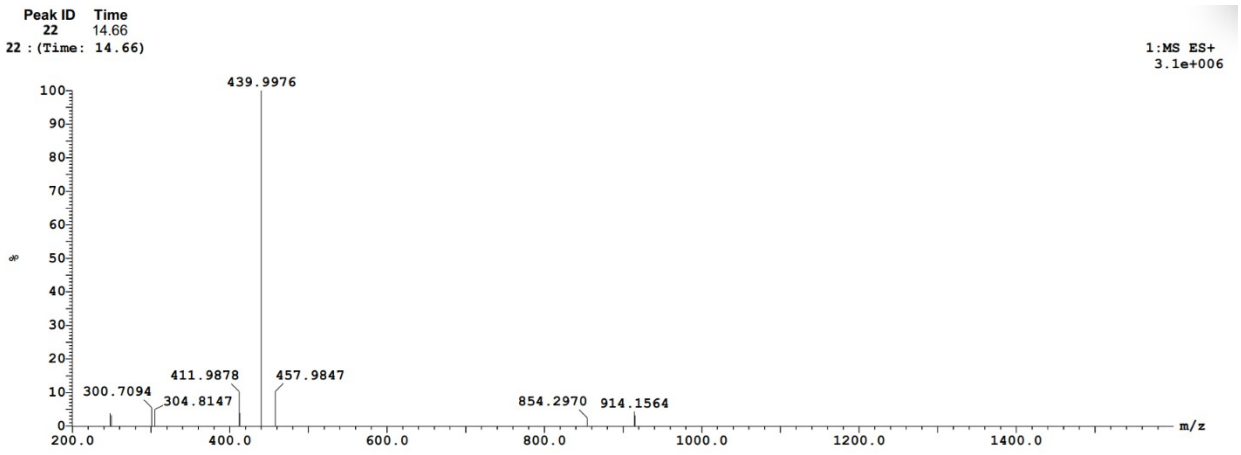

Fig. S.22. Peak 22 MS/MS fragmentation

2.2. Structure elucidation of isolated compounds of the butanol fraction

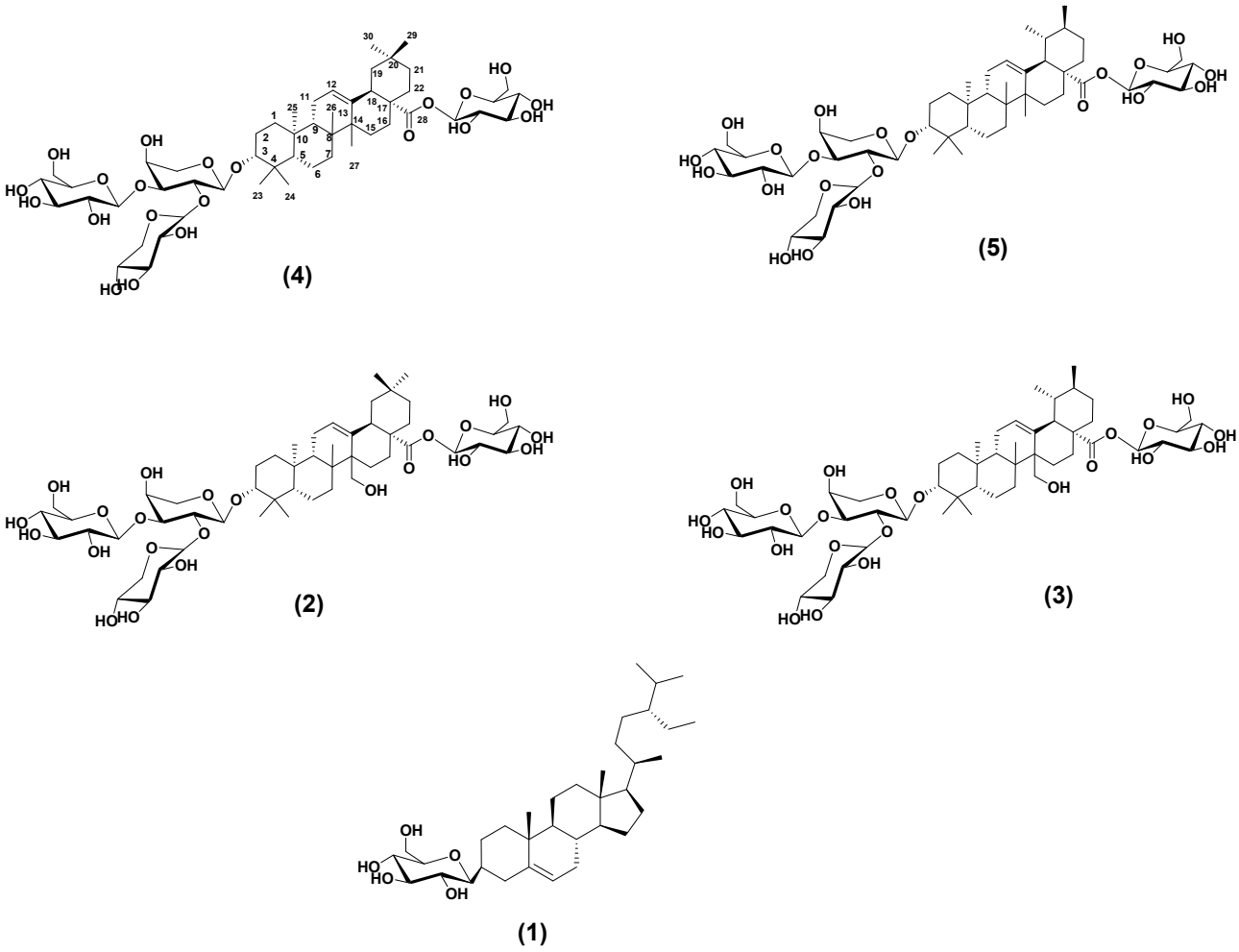

Fig. S.23. Structures of the isolated and identified saponins from *F. arabica* L. butanol fraction; **(1)**: *β*-sitosterol glucoside, **(2)**: 3-*β*-D-D-xylopyranosyl(1→2)-[*β*-D-glucopyranosyl (1→3)]-*α*-L-arabinopyranosyl 27-hydroxyoleanolic acid, 28-*O*-*β*-D-glucopyranoside, **(3)**: 3-*O*-*β*-D-xylopyranosyl (1→2)-[*β*-D-glucopyranosyl (1→3)-*α*-L-arabinopyranosyl 27-hydroxyursolicacid 28-*O*-*β*-D-glucopyranoside , **(4)**: 3-*O*-*β*-D-xylopyranosyl(1→2)-[*β*-D-glucopyranosyl(1→3)]-*α*-L-arabinopyranosyl oleanolic acid 28-*O*-*β*-D-glucopyranoside , and **(5):** 3-*β*-D-xylopyranosyl(1→2)-[*β*-D-glucopyranosyl(1→3)]-*α*-L-arabinopyranosyl ursolic acid 28-*O*-*β*-D-glucopyranoside.

Table S.2. ^{1}H (400 MHz) and ^{13}C NMR data (101 MHz) for compound **1** in pyridine-d_5.

No.	δ_H (J in Hz)	δ_c	APT	HMBC
1	0.97, 1.73 m	37.27	CH_2	
2	1.30, 1.76 m	30.05	CH_2	
3	3.93, m	78.28	CH	
4	2.47 t, 2.71 d (13.4)	39.13	CH_2	
5		140.70	C	
6	5.34 d, (5.3)	121.71	CH	
7	1.52 m, 1.86 m	31.96	CH_2	
8	1.91 m	31.84	CH	
9	0.89 m	50.13	CH	C-10
10		36.71	C	
11	0.90 m, 1.42 m	21.06	CH_2	
12	1.95 m, 1.90 m	39.73	CH_2	
13		42.26	C	
14	0.93 m	56.60	CH	
15	1.28 m	24.29	CH_2	
16	1.83 m	28.33	CH_2	
17	1.10 m	56.03	CH	
18	0.64, s	11.76	CH_3	C-12, C-13, C-14, C-17
19	0.92, s	19.21	CH_3	C-1, C-5, C-9, C-10
20	1.37 m	36.17	CH	
21	0.97, d (6.4)	18.79	CH_3	C-17, C-20, C-22
22	1.06 m, 1.38 m	33.99	CH_2	
23	1.24 m	26.84	CH_2	
24	0.98 m	45.83	CH	
25	1.96 m	29.25	CH	
26	0.85, d, 7.4	19.76	CH_3	C-24, C-25, C-27
27	0.83, d, 7.6	18.99	CH_3	C-24, C-25, C-26
28	0.90 m, 1.07 m	23.18	CH_2	
29	0.87, t, 7.5	11.94	CH_3	C-24, C-28
3-*O*-*β*-D-glucopyranose				
1`	5.05, d, 7.6	102.37	CH	
2`	4.05, t, 7.9	75.14	CH	
3`	4.29, m	78.41	CH	
4`	7.27, m	71.49	CH	
5`	3.97, m	77.89	CH	
6`a 6`b	4.56, brd, 10.9 4.41, dd, 11.3, 4.8	62.63	CH_2	

Table S.3 ^{1}H (400 MHz) and ^{13}C NMR data (101 MHz) for compound **4** in pyridine-d_5.

Position	APT	δ_C	δ_H
1	CH_2	38.7	0.87 (a) 1.48 (e) (m, overlapped)
2	CH_2	26.5	1.82 (a) 2.08 (e)
3	CH	89.0	3.24 (dd, *J* = 11.7, 4.4 Hz, 2H)
4	C	39.7	-
5	CH	55.8	0.77 (m)
6	CH_2	18.3	1.32 (a) 1.48 (e)
7	CH_2	32.3	1.75 (m)
8	C	39.9	-
9	CH	47.8	1.59 (dd, *J* = 16.9, 6.5 Hz)
10	C	36.8	-
11	CH_2	23.8	1.98 (m)
12	CH	123.0	5.43 (m)
13	C	143.9	-
14	C	41.9	-
15	CH_2	28.4	1.15 (a) 2.42 (e)
16	CH_2	23.2	2.08 (a) 1.87 (e)
17	C	48.1	-
18	CH	41.5	3.15 (m)
19	CH_2	46.8	1.20 (a) 1.74 (e)
20	C	29.7	-
21	CH_2	34.2	1.01 (m)
22	CH_2	33.3	1.32 (a) 1.48 (e)
23	CH_3	27.6	1.26 (s)
24	CH_3	17.4	1.12 (s)
25	CH_3	15.5	0.85 (s)
26	CH_3	16.3	1.08 (s)
27	CH_3	25.9	1.23 (s)
28	C	176.2	-
29	CH_3	32.9	0.89 (s)
30	CH_3	23.4	0.86 (s)

Table S.4. ^{13}C NMR chemical shifts of sugar moieties of saponin **4** in pyridine-d_5 (ppm)

C	δc	δ_H
3-*O*-Arabinose		
1	105.5	4.73 (d, *J* = 7.2 Hz)
2	77.2	4.66 (dd, *J* = 9.1, 7.2 Hz)
3	83.8	4.26
4	68.8	4.49
5	66.0	3.62
3-*O*-Xylose		
1	104.9	5.39 (d, *J* = 7.7 Hz)
2	75.2	3.99
3	78.9	4.10
4	71.3	4.20
5	66.9	3.43 (t)
3-*O*-Glucose		
1	104.9	5.30 (d, *J* = 7.7 Hz)
2	75.1	4.02
3	78.6	4.28
4	70.9	4.35
5	78.2	3.92
6	62.3	4.32
28-*O*-Glucose		
1	95.5	6.32 (d, *J* = 8.1 Hz)
2	73.8	4.20
3	78.2	4.21
4	70.7	3.61
5	79.17	4.02
6	62.1	4.44

Table S.5. ^{13}C-NMR shifts for differentiating oleanolic and ursolic acid and their 27-hydroxy analogues in pyridine-d_5 (ppm)

C	Oleanolic acid	Ursolic acid	27-OH Oleanolic	27-OH Ursolic
12 (CH)	123.8	123.8	129.8	131.2
13 (C)	143.9	135.8	138.2	138.2
14 (C)	40.7	41.0	46.0	48.1
15 (CH_2)	29.7	29.7	26.5	26.5
17 (C)	47.0	47.9	48.1	48.1
18 (CH)	41.5	53.1	41.5	53.1
19	46.8 (CH_2)	39.1 (CH)	46.8 (CH_2)	39.1 (CH)
20	29.7 (C)	39.1 (CH_3)	30.5 (C)	39.1 (CH_3)
21 (CH_2)	35.2	29.7	33.3	30.5
22 (CH_2)	32.3	36.9	32.3	36.8
27 (CH_3)	25.9	23.6	64.2	64.2
29 (CH_3)	33.3	17.7	32.9	18.0
30 (CH_3)	23.4	21.1	23.6	21.1

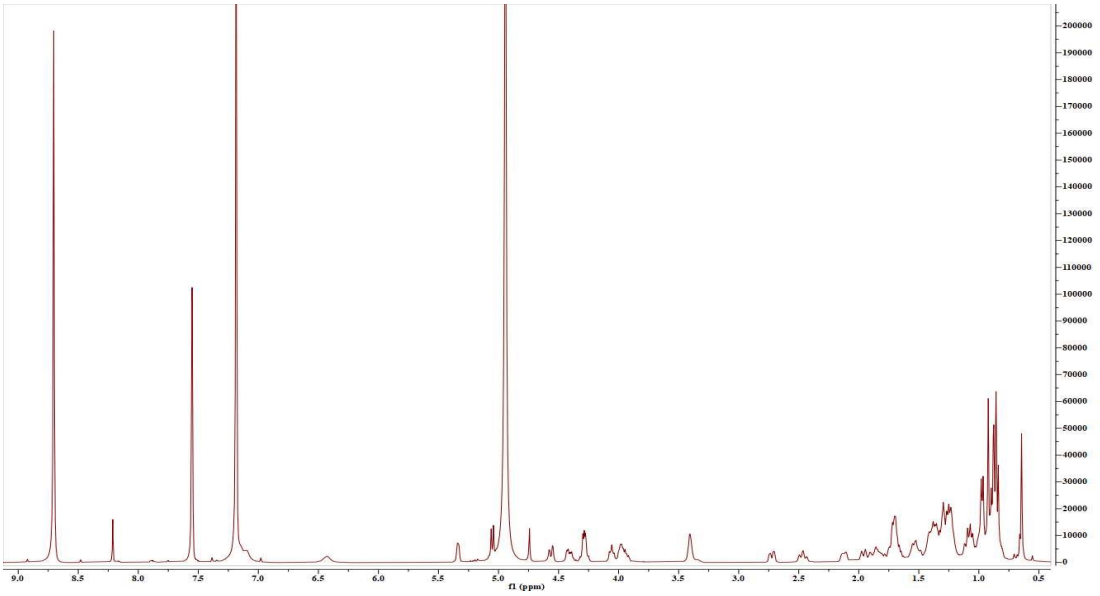

Fig. S.24. ^{1}H (400 MHz) for compound **1** in pyridine-d_5.

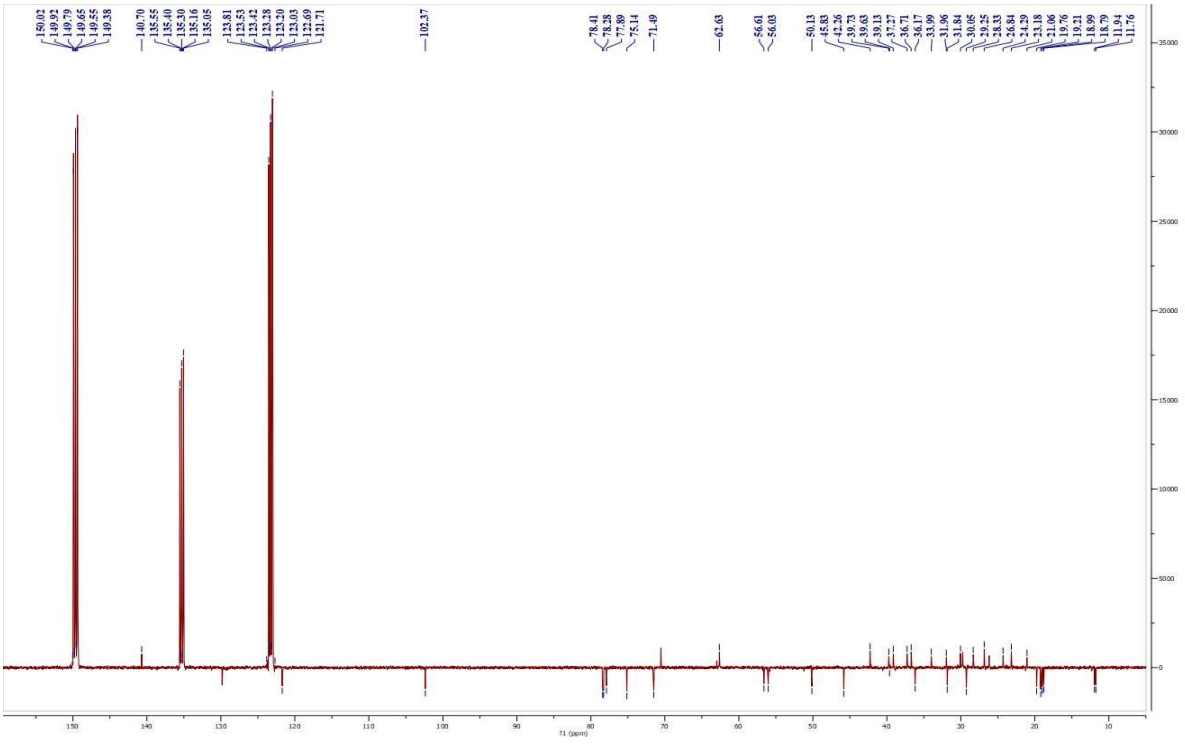

Fig. S.25. ^{13}C NMR data (101 MHz) for compound **1** in pyridine-d_5

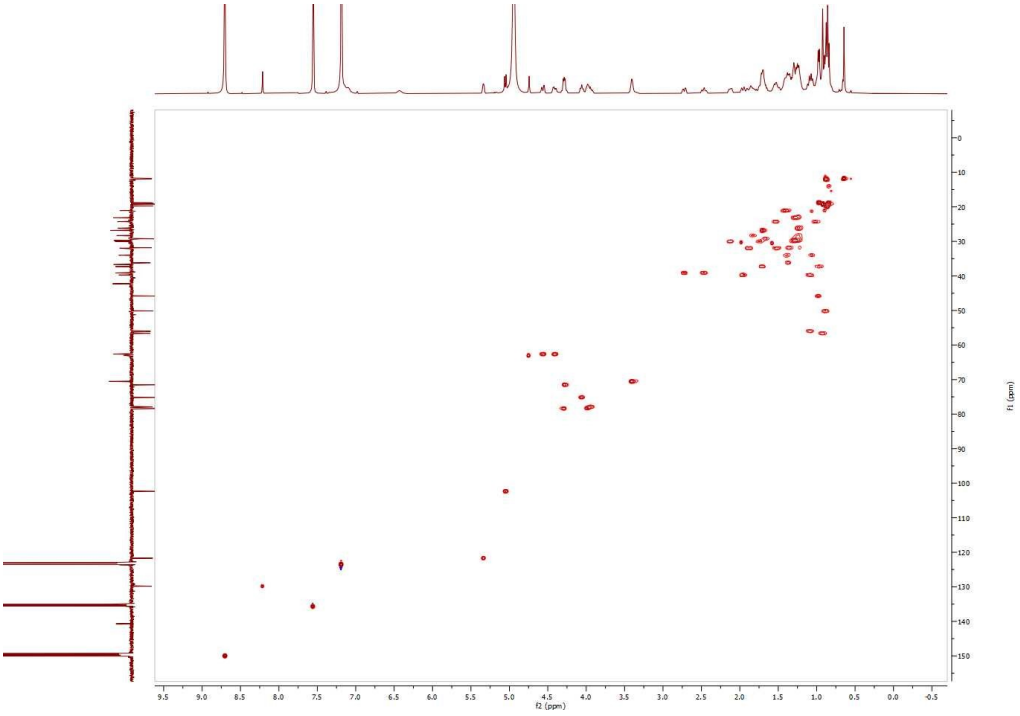

Fig. S.26. HSQC data for compound **1** in pyridine-d_5

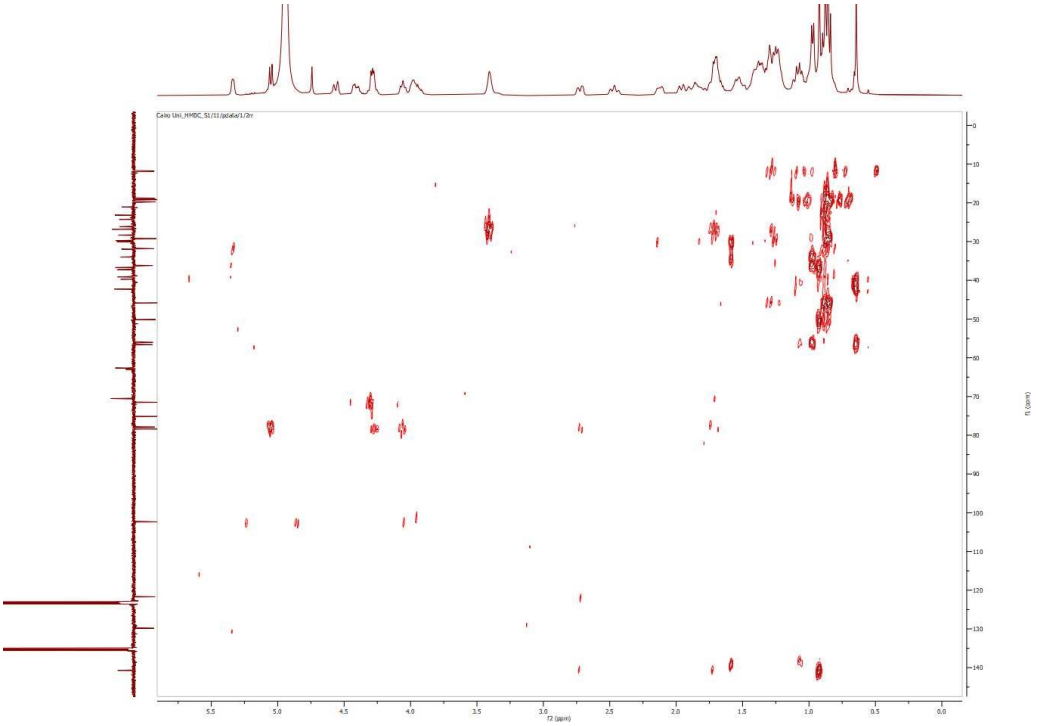

Fig. S.27. HMBC data for compound **1** in pyridine-d_5

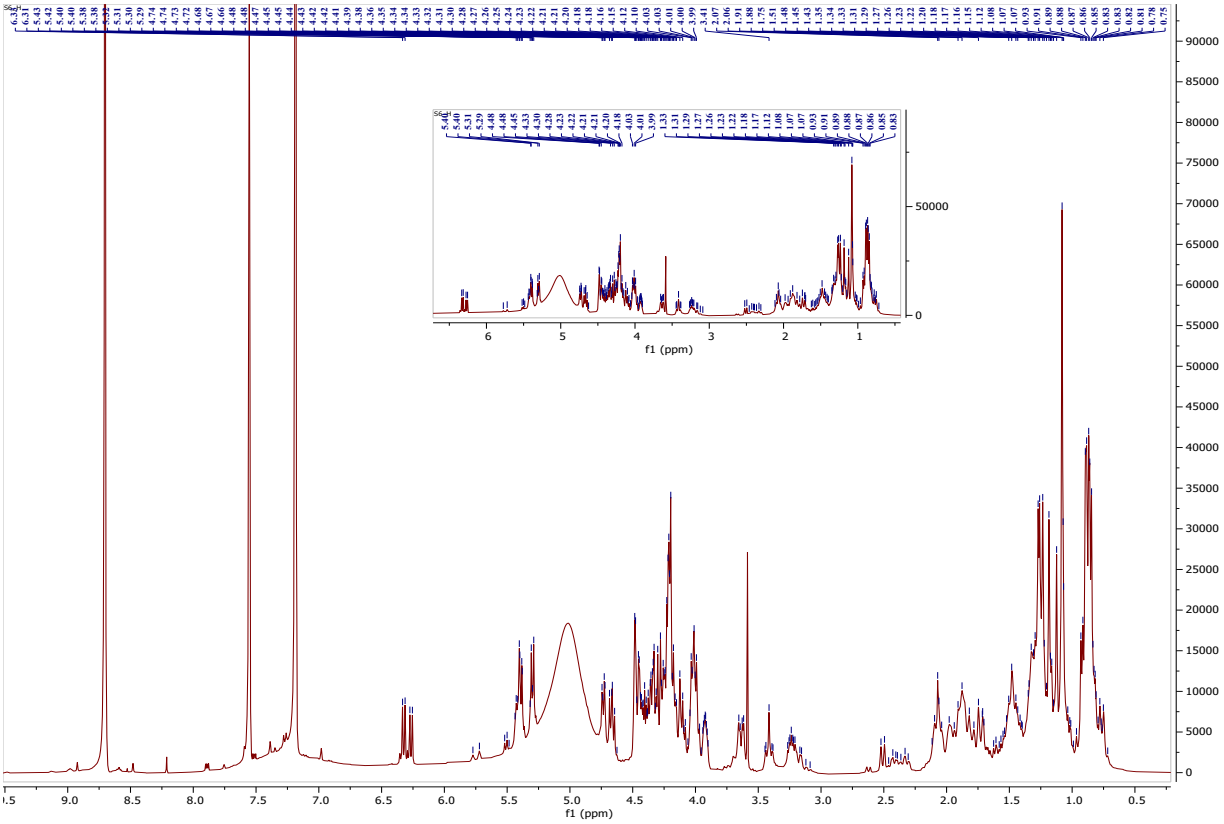

Fig. S.28. ^{1}H (400 MHz) for a mix of compounds **2** and **3** in pyridine-d_5.

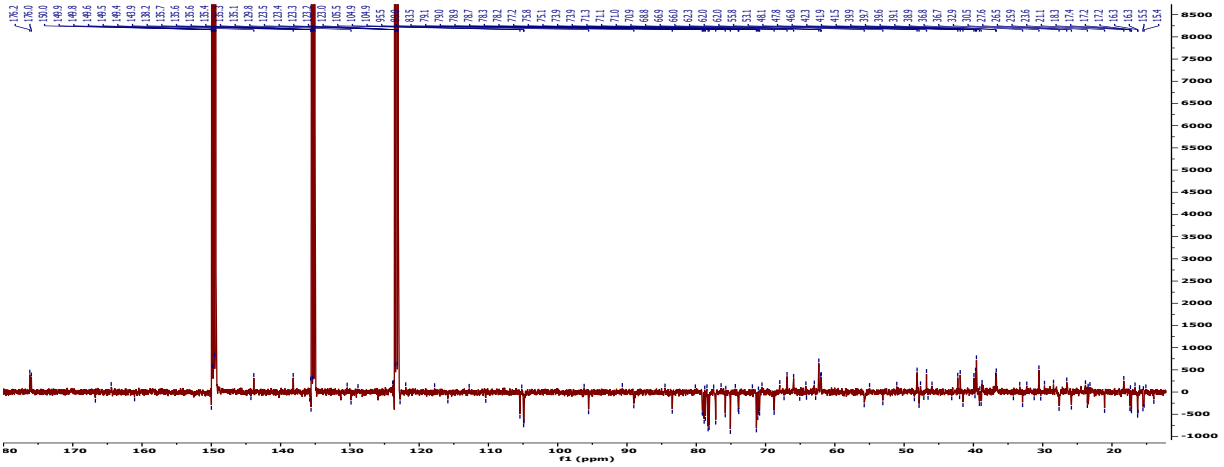

Fig. S.29. ^{13}C NMR data (101 MHz) for a mix of compounds **2** and **3** in pyridine-d_5

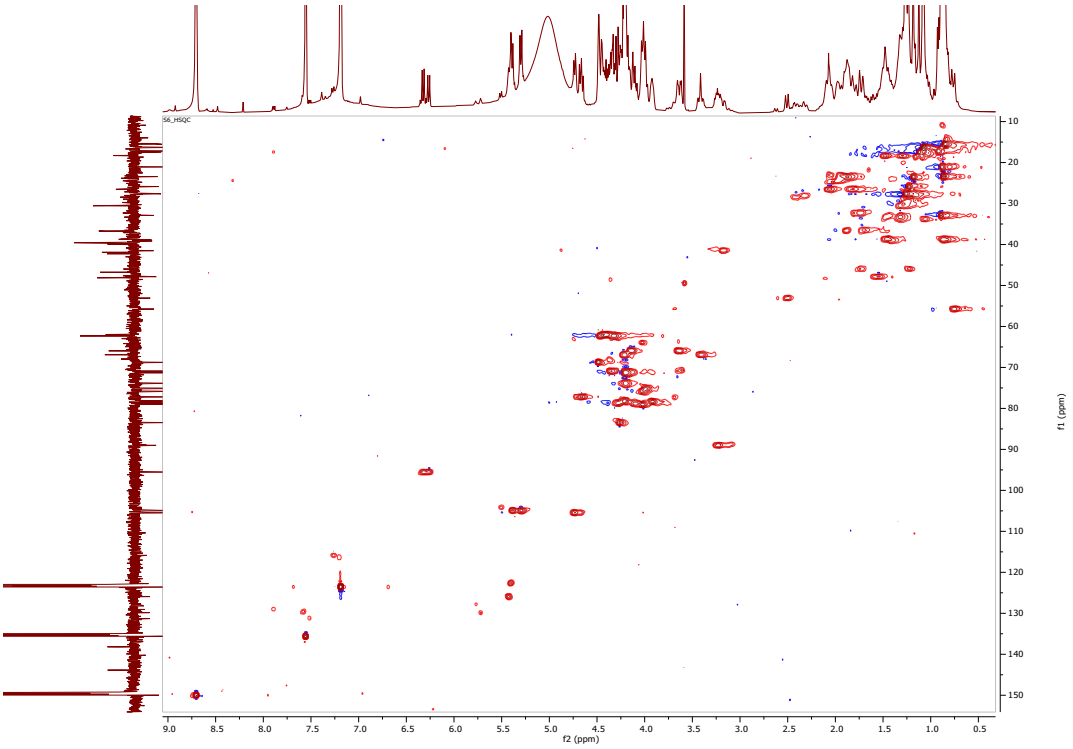

Fig. 30. HSQC data for a mix of compounds **2** and **3** in pyridine-d_5

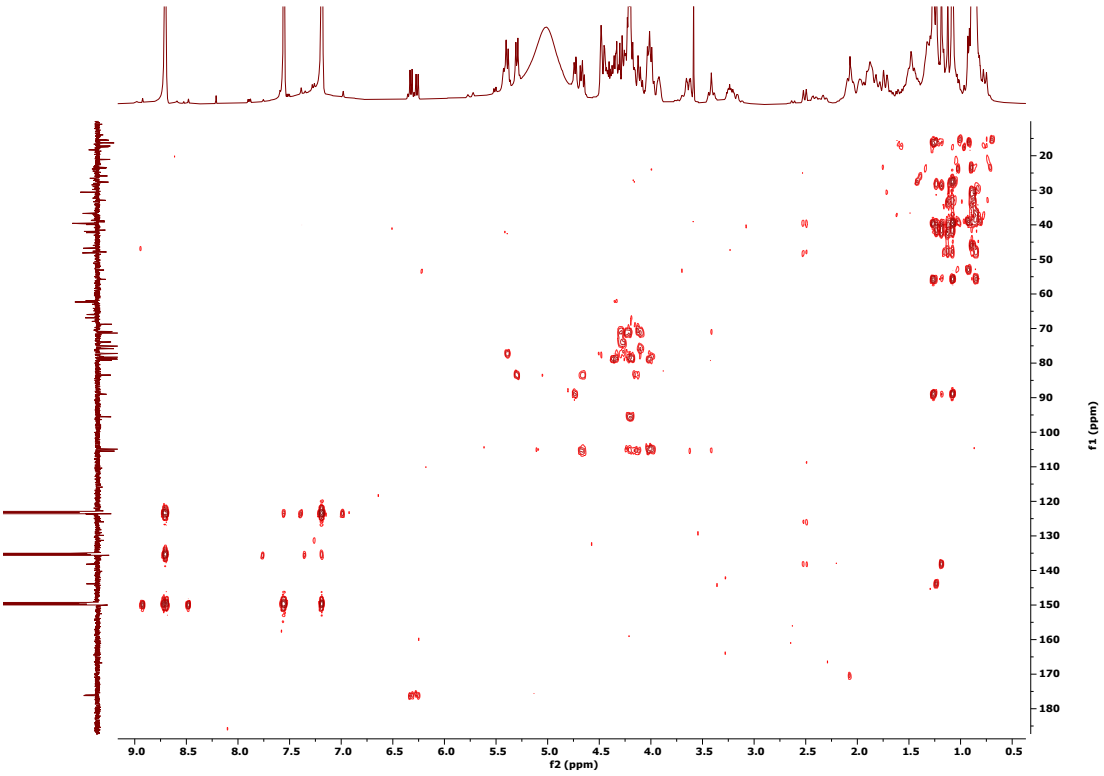

Fig. 31. HMBC data for a mix of compounds **2** and **3** in pyridine-d_5

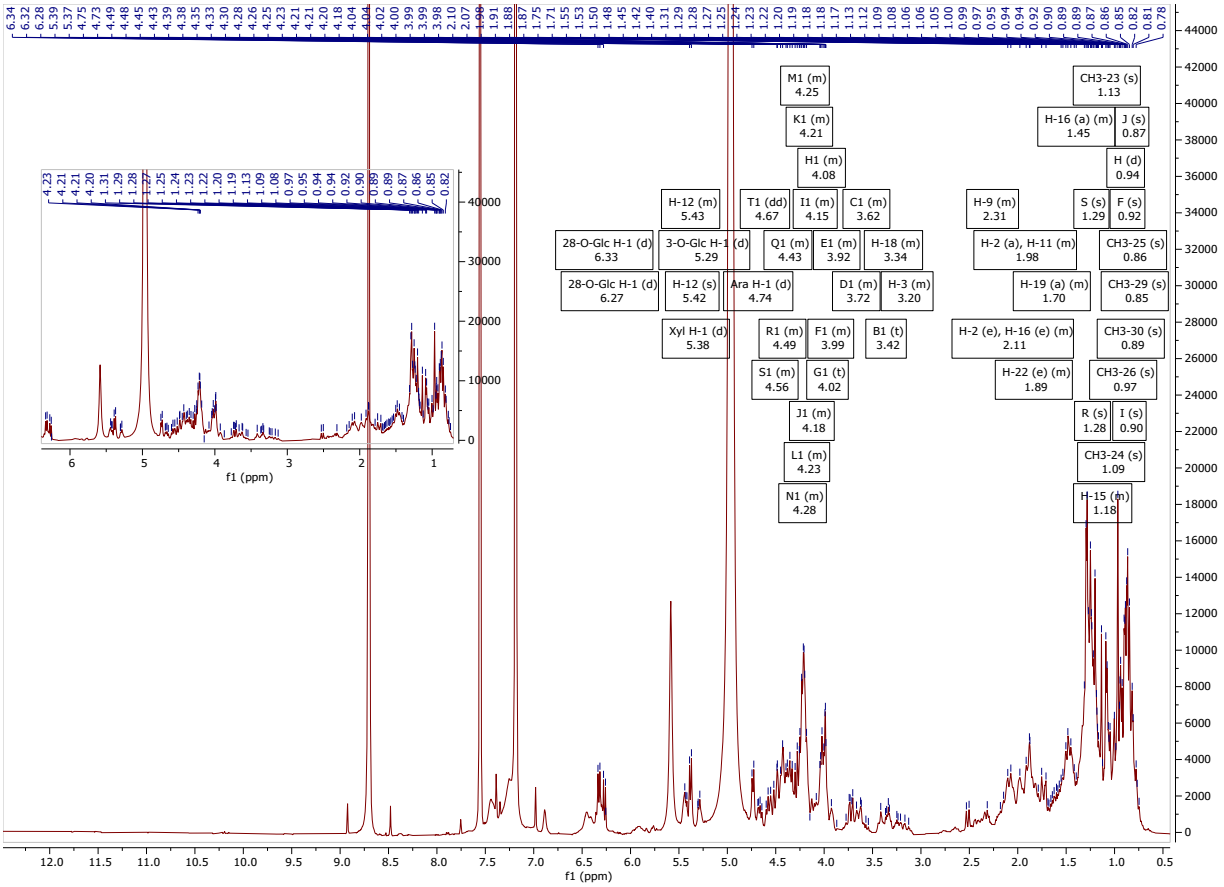

Fig. S.32 ^{1}H (400 MHz) for a mix of compounds **4** and **5** in pyridine-d_5.

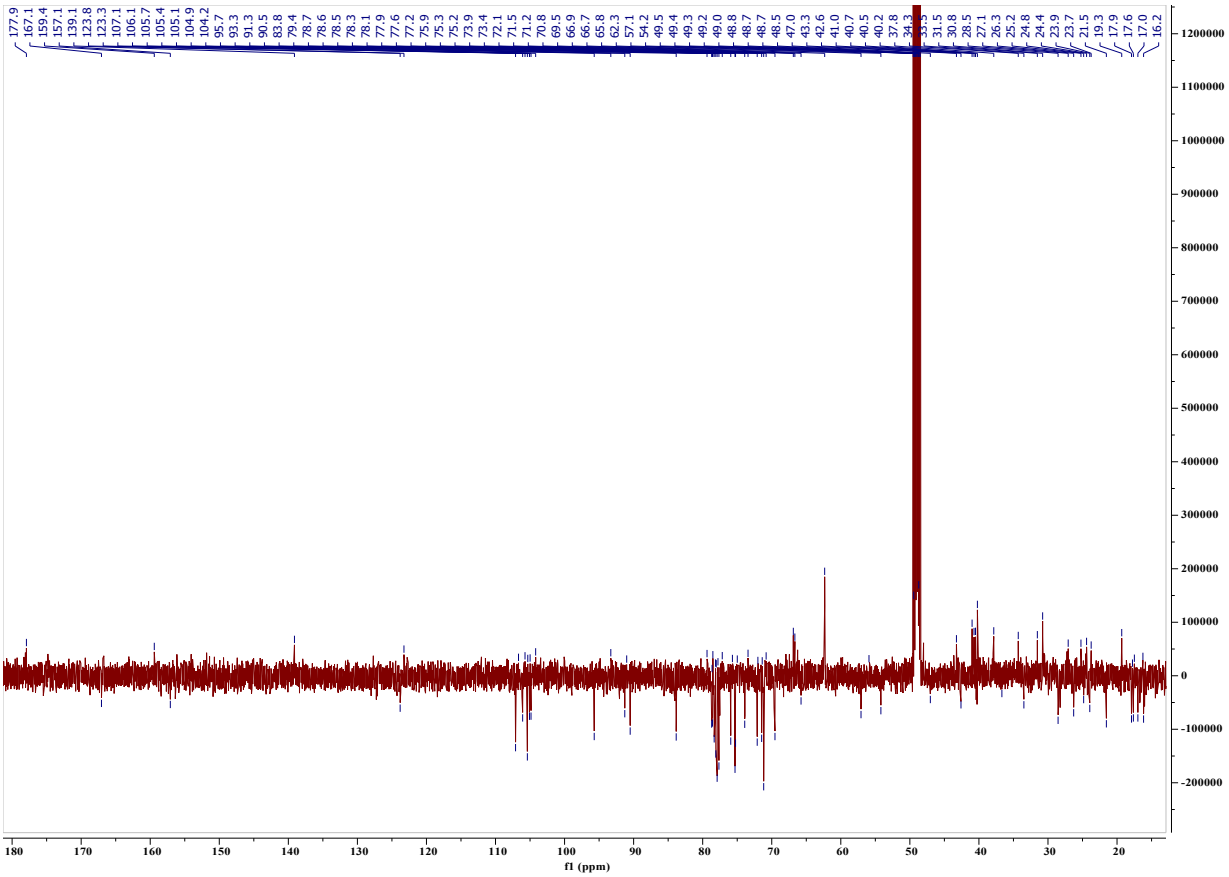

Fig. S.33 (a) ^{13}C NMR data (126 MHz) for a mix of compounds **4** and **5** in CD_3OD

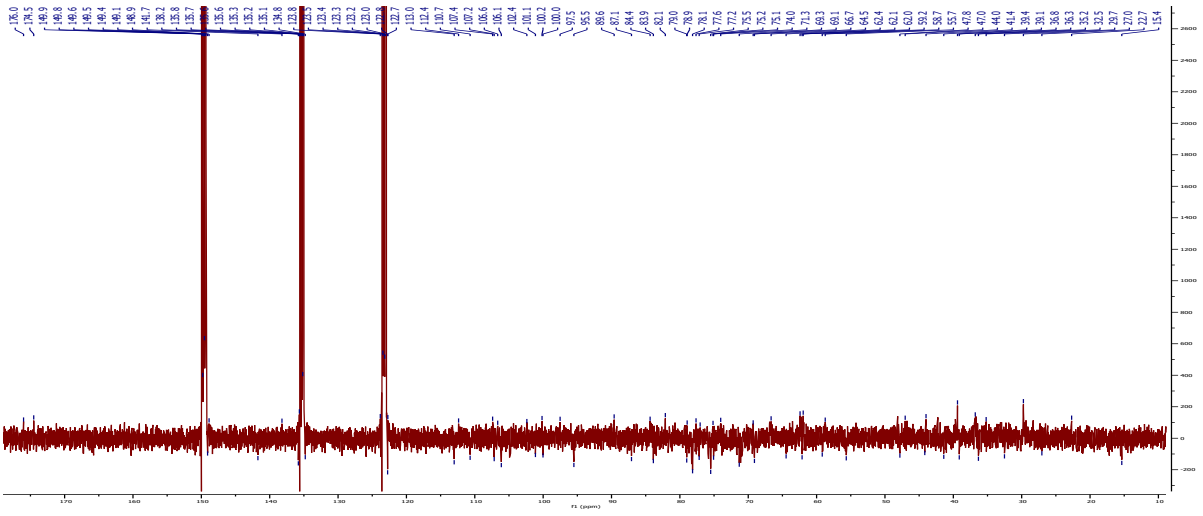

Fig. S.33 (b) ^{13}C NMR data (101 MHz) for a mix of compounds **4** and **5** in pyridine-d_5